Khasmaral et al. Mongolian Geoscientist 49 (2019) 3-21
https://doi.org/10.5564/mgs.v0i49.1223

Mongolian Geoscientist

Original article

Geochemical comparison of late Mesozoic and early Cenozoic volcanic rocks in South Mongolia: Implications for petrogenesis and geodynamic evolution

Togtokh Khasmaral[1,2*], Bars Amarjargal[1,5], Laicheng Miao[1,2], Baatar Munkhtsengel[3], Anaad Chimedtseren[3]

[1]*Key Laboratory of Mineral Resources, Institute of Geology and Geophysics, Chinese Academy of Sciences, Beijing 100029, China*
[2]*Institutions of Earth Science, Chinese Academy of Sciences, Beijing 100029, China*
[3]*Department of Geology and Hydrogeology, School of Geology and Mining, Mongolian University of Science and Technology, Ulaanbaatar 14191, Mongolia*
[4]*Dald Erdene Mongolia LLC, Ulaanbaatar 14190, Mongolia*
[5]*Underground Geosciences Services Department, Oyutolgoi LLC, Ulaanbaatar 14240, Mongolia*

**Corresponding author. Email: khasmaral@wealthmon.mn*

ARTICLE INFO

***Article history*:**
Received 10 September 2019
Accepted 11 October 2019

ABSTRACT

The Mesozoic-Cenozoic volcanic rocks are widely distributed in the interior of the East Asia and document the tectonic transition of East Asia. We present new geochronology and geochemistry data of late Cretaceous-early Cenozoic basalts in Bayantsagaan and Han-Uul volcanic provinces in South Mongolia, in order to explore their petrogenesis and geodynamic settings. The volcanic rocks in the Bayantsagaan and Han-Uul field yielded K-Ar ages of 90.55±1.93 Ma and 55.49±1.49 Ma, respectively. The volcanic rocks in South Mongolia subdivided into to alkaline basalts and tholeiitic series, and are characterized by ocean island basalts (OIB) trace elements features, such as enrichment of light REE relative to heavy REE and enrichment in large ion lithophile elements (LILE). Compared with the late Cretaceous, the early Cenozoic basalts show an increase of Nb and Ta. Crustal contamination and fractional crystallization are insignificant in the genesis of late Cretaceous and early Cenozoic basalts South Mongolia. The available Sr-Nd isotope results indicate that late Cretaceous volcanic rocks, which derived from magmas from the of metasomatized subcontinent lithospheric mantle, whereas the early Cenozoic basalts is ascribed to contributions from the asthenospheric mantle. We propose that the generation of the late Cretaceous volcanic rocks (114-90 Ma) related back arc-extension induced by slab rollback of the westward-subducted Pacific Plate and the subduction zone retreat. Whereas Early Cenozoic volcanism (50-40 Ma) in Mongolia is related to the shallow mantle upwelling (asthenosphere) induced by the edge convection along the northern margin of the North China Craton (NCC), triggered by a far-field effect of Indo-Asian collision.

Keywords: Bayantsagaan, Han-Uul field, mantle upwelling

INTRODUCTION

The volcanic rocks of Mesozoic-Cenozoic age are distributed over a vast region from the coastal area of East Asia continent and in the interior of the East Asia continent, such as Mongolia as well.

Mesozoic volcanism in Mongolia is mainly emplaced during the late Jurassic-early Cretaceous, and late Cretaceous volcanism was mainly distributed in East Mongolia and South Mongolia. Several studies have been carried out for late Mesozoic volcanic rocks in East

© The Author(s). 2019 **Open access** This article is distributed under the terms of the Creative Commons Attribution 4.0 International License (https://creativecommons.org/licenses/by/4.0/), which permits unrestricted use, distribution, and reproduction in any medium, provided you give appropriate credit to the original author(s) and source, provide a link to the Creative Commons license, and indicate if changes were made.

Mongolia, demonstrated that bimodal series arc type volcanic rocks migrates from west to east with time. Their origin was linked to the back-arc extension induced by slab rollback of the westward-subducted Pacific Plate (Dash et al., 2013; Bars et al., 2018).

In contrast, South Mongolian volcanic rocks are isolated in space and have relatively smaller outcrop which is erupted both late Cretaceous and Early Cenozoic. Despite few studies of their geochemistry (Barry and Kent, 1998; Yarmolyuk et al., 2015), there is still great controversy on the origin of these basalts. It is noted that the "Big Mantle Wedge" (BMW) model has been widely accepted in interpreting the geodynamic setting of the Cenozoic volcanism in East Mongolia and East China (e.g., Zhao et al., 2009; Kuritani et al., 2011; Togtokh et al., 2018; Xu et al., 2012; Zhang et al., 2014; Xu and Zheng et al., 2017). However, it will be difficult to use the BMW model to explain the petrogenesis and geodynamic setting of the basalts in Mongolia, especially those in South Mongolia, since South Mongolia is about 2000 km west of the present Pacific trench, which is too far to correlate the volcanic rocks there to the Pacific subduction. Alternatively, some researchers (Barry et al., 2003) believe that OIB-like late Cretaceous- Early Cenozoic basalts in South Mongolia have the same origin as late Cenozoic volcanic rocks in Central Mongolia.

In this paper, we present new geochemical and geochronological data of the Cretaceous -early Cenozoic basalts in South Mongolia. Using these results, together with previously published data, we explore the petrogenesis and discuss the geodynamic setting in which the late Cretaceous- early Cenozoic volcanism occurred in South Mongolia.

GEOLOGICAL BACKGROUND

Mongolia is located within the central part of the CAOB (Jahn et al., 2004). The basement geology of Mongolia records a complex history of Paleozoic terrane accretion and arc magmatism of the Central Asian Orogenic Belt (CAOB), with a general southward migration to the Sulinkheer suture, which marks the final closure of the Paleo-Asian Ocean in the late Permian to the Early Mesozoic (Sengor and Natal'in, 1996; Miao et al., 2008; Xiao et al., 2010). The Mongol-Okhosk belt (MOB) extends from the central Mongolia in the west to Uda Golf in the east, result of a scissor-style closure of the Mongol-Okhotsk Ocean during Middle Jurassic in the Mongolian segment (e.g., Tomurtogoo et al., 2005; Miao et al., 2017). The Indo-Asian collision and/or the western Pacific subduction likely influenced the Central-Eastern Mongolia in a manner of the far-field stress during Cenozoic, leading to the present geography and formation/ reactivation of NE- to NNE-trending faults and rifting basins (e.g., Yin, 2010). Mesozoic to Cenozoic basalts are widely distributed in east and central Mongolia (Fig. 1). Mesozoic volcanic rocks in East Mongolia erupted during late Jurassic-Early Cretaceous (ages ranging from ca. 155 to 99 Ma), essentially coeval with those of the adjacent Great Xing'an Range of NE China continent (e.g., Pei et al., 2008; Dash et al., 2013; Bars et al., 2018), whereas other basalts were formed in South Mongolia during 114 to 90 Ma. In contrast to the Mesozoic basalts of East Mongolian, the late Cretaceous volcanism in south Mongolia relatively are scattered over large area, where the early Cenozoic volcanic complex of 60-50 Ma were also distributed (Enkhtuvshin et al., 1995; Barry et al., 2003; Yarmolyuk et al., 2015). Except for the "old" field above mentioned, the Cenozoic volcanic rocks in Mongolia with ages younger than 30 Ma are more widespread.

SAMPLING AND PETROGRAPHY

In this study, 14 fresh samples were collected from two localities in South Mongolia.

Detailed localities of samples are shown in Fig. 1.

Bayantsagaan volcanic fields are located at southern edge of Gobi-Altai ranges and overlie the middle Jurassic Saihan Formation (Fm) (Fig. 2a). Volcanic rocks mainly consist of black and massive trachybasalts. The lavas thickness is 250–300 m in total. Lavas have oxidized upper surface, with ropey texture or columnar jointing in thicker lavas (Fig. 2b). Bayantsagaan trachybasalts are porphyritic and contain phenocrysts of predominant

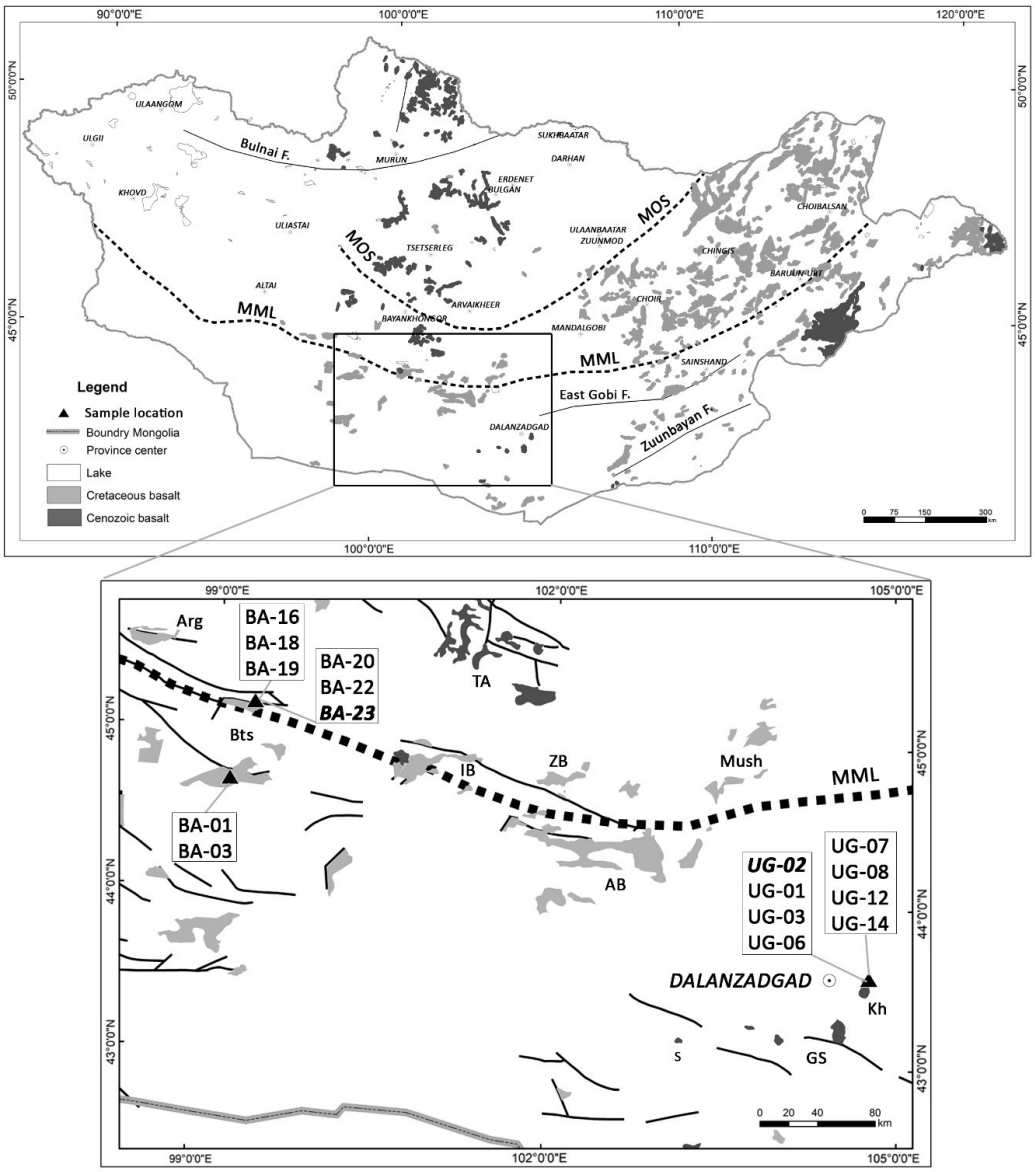

Fig. 1. Simplified tectonic outline and distribution of Mesozoic-Cenozoic volcanic rocks in Mongolia (modified after Yarmolyuk et al., 2011, Barry, 1999). Sample localities and numbers of this study also showed. MOS: Mongol-Okhotsk suture; MML: Main Mongolian Linement. Abbreviation names are as follows: Arg-Argalant; Bts-Bayantsagaan; IB-Ikh bogd; ZB-Zuunbogd; AB-Ajbogd; Mush-Mushgai; Kh-Han-Uul; GS-Gurvansaikhan; TA-Taatsiin gol

plagioclase and subordinate actinolite, which scatter in a groundmass, composed of acicular plagioclase and minor amount clinopyroxene (Fig. 3a). Plagioclase phenocrystal (Pl) is euhedral to subhedral, and 0.5-1.5 mm in size. Actinolite (Hb) occur as elongated acicular, subhedral grains of up to 0.5 mm in size (Fig. 3b).

The Han-Uul volcanic field is located at the eastern termination of the Gobi Tien Shan ranges. The Cenozoic basaltic lava in this volcanic field occurs as a plateau overlying the lower Cretaceous Sainshand Fm (Fig. 2c). There are at least three lava flows, with each 8-28 m thick. These lava flows are similar in lithology and consist mainly of pale gray, black massive basalt and trachybasalt. They show massive, horizontally bedded layers (Fig. 2d). No volcanic craters were identified as the conduit of these lavas. The Cenozoic volcanic rocks in this field were designated as Eocene in age but no age data available. Consequently, besides the

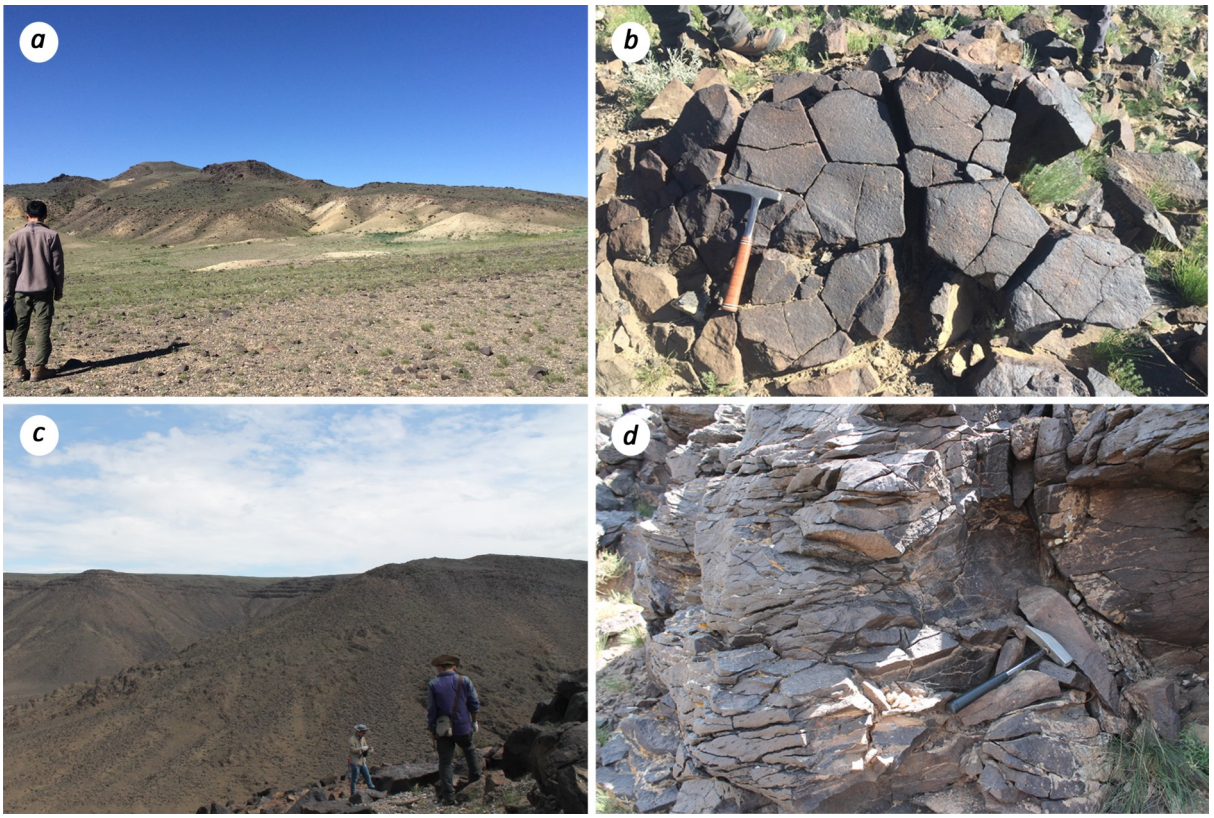

Fig. 2. Field photo (a) basaltic lava flow overlying sediments with a bedding structure in the Bayantsagaan volcanic field, (b) vertical columnar joints in lava Bayantsagaan volcanic field, (c) lava flows forming a plateau unconformably overlying the Upper Cretaceous Sainshand Fm, and (d) massive blocky surface of the basaltic lava at the Han-Uul area

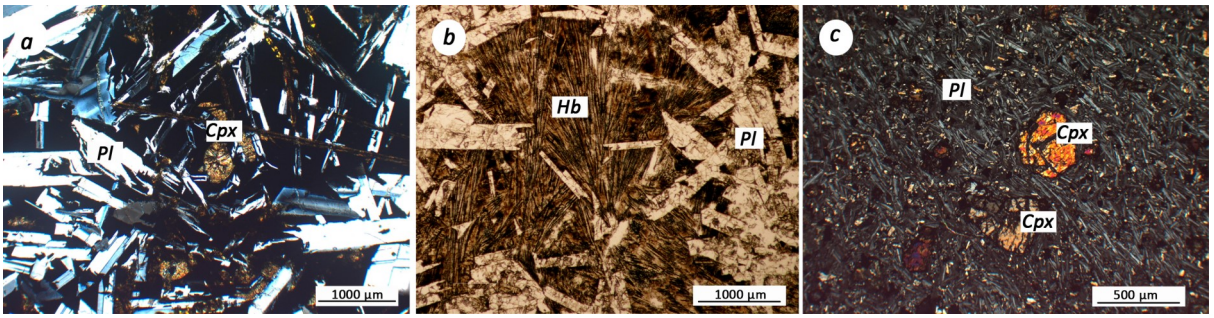

Fig. 3. Photomicrograph (cross-polarizers) showing: (a) clinopyroxene phenocrysts surrounded by plagioclase laths in basaltic andesite from the Bayantsagaan volcanic field (sample BA-01), (b) subhedral acicular Actinolite cryst in the basaltic andesite from the Bayantsagaan volcanic field (sample BA-19), (c) Foliation structure in basalt from Han-Uul volcanic field (UG-03). Abbreviations: Pl – plagioclase; Cpx – clinopyroxene; Hb-hornblende

samples for geochemical analysis, one sample (UG-02) from the lower part of the volcanic sequence was collected for age dating in this study. The basalts from the Han-Uul volcanic field are vesicular and porphyritic. Olivine (Ol) is the most common phenocryst phase; although clinopyroxene phenocrysts are, also present. Olivine phenocrysts are euhedral to subhedral prisms of 0.4-2 mm in size. The groundmass consists of olivine, clinopyroxene, plagioclase microlites and volcanic class. The Han-Uul basaltic lavas display magmatic foliation structure, which is characterized by alignment and orientation of tiny plagioclase laths in the groundmass, as well as by the variation of the foliation surrounding the clinopyroxene

phenocrysts (Fig. 3c). This suggests that the foliation records primitive magma flowing.

ANALYTICAL METHODS

Whole-rock K-Ar dating

Whole rock K-Ar dating was carried out at the State Key Laboratory of Earthquake Dynamics, Institute of Geology, Chinese Earthquake Administration (IGCEA, Beijing, China). Rocks were crushed and sieved through 20-80 mesh in size, cleaned with distilled water, ethanol and acetone, and baked at low temperature. After cleaning and baking, samples were enclosed in a "Christmas tree" shaped holder and heated at about 200°C for 12 hour for degassing. Afterward samples were separated and placed in individual molybdenum crucibles surrounded by a titanium crucible for electron bombardment heating. Argon was measured using the isotope dilution method with a 99.98% pure ^{38}Ar spike on a MM120 mass spectrometer connected to a purification and extraction system. The spike was calibrated and corrected with standard samples. Detailed analytical procedures were described by Zhu et al. (2001).

Whole-rock major and trace element analysis

Major and trace element analyses were carried out at the Institute of Geology and Geophysics, Chinese Academy of Sciences in Beijing, China. Fresh rock samples crushed and milled to 200 mesh. 0.5 g whole-rock powders were accurately weighed and then ignited at 1000°C for about 60 min. Loss on ignition (LOI) was measured as the weight loss after ignition. Samples were then grinded and mixed with 5 g of lithium tetraborate ($Li_2B_4O_7$) in an agate mortar, and melted to make glass discs using an automatic flame fusion machine. Major elements were determined on fused glass discs by X-ray fluorescence spectroscopy (XRF) using an Axios-Minerals instrument. The analysis has a relative standard deviation (RSD) of 0.1–1.0%. For trace elements, sample powders were digested using a hot mixture of HF and HNO_3 in the high pressure Teflon bombs for 7 days. The concentrations of trace elements were determined by using an inductively coupled plasma mass spectrometry (ICP-MS) of Finnigan MAT Element-II system. Detailed analytical procedures were described in (Guo et al., 2006).

Whole-rock Sr-Nd isotope analysis

Rb–Sr and Sm–Nd isotopic compositions were determined by thermal ionization mass spectrometry (TIMS) using a Finnigan MAT262 at the Institute of Geology and Geophysics, Chinese Academy of Sciences in Beijing, China. System following the procedures are described in Guo et al. (2006) and Li et al. (2012a). Whole -rock powders for Sr–Nd isotope analyses were dissolved in Savillex Teflon screw-top capsule after being spiked with the mixed ^{87}Rb –^{84}Sr and ^{149}Sm –^{150}Nd tracers prior to HF + HNO_3 + $HClO_4$ dissolution. Rb, Sr, Sm and Nd were separated using the classical two-step ion exchange chromatographic method before determination by the TIMS technique. The blank was lower than 250 pg for Rb–Sr and 100 pg for Sm–Nd, respectively. International standards NBS-987 and JNdi-1 of USGS were employed to evaluate instrument stability during the period of data collection.

RESULTS

Whole-rock K-Ar ages

K-Ar dating results of two samples are presented in Table 1. Sample 2014BA-23 from Bayantsagaan gave an age of 90.55±1.93 Ma, and the Han-Uul (2014UG-02) yielded an age of 55.49±1.49 Ma.

Major and trace element composition

Major and trace element compositions of analyzed samples are presented in Table 2. In total alkali vs. silica (TAS) diagram, the Bayantsagaan volcanic rocks plot in the field of basaltic andesite. Following the classification of Irvine and Baragar (1971), these samples are subdivided into alkaline and tholeiitic groups. Volcanic rocks from Han-Uul fall in fields of basalt and trachybasalt, belonging to alkaline (Fig. 4).

Volcanic rocks from Han-Uul fields have the higher MgO contents of 6.11-9.90 wt % (on water-free basis, hereinafter), whereas those from Bayantsagaan have lower MgO contentsof 3.36-4.86 wt%. Han-Uul volcanic rocks have

Table 1. Whole rock K-Ar dating result of Bayantsagaan and Han-Uul volcanic rocks from South Mongolia

Sample No.	Location	^{40}Ar	K%	Age±σ（Ma）	^{40}Ar%	^{40}Ar(mol/g)
2014UG-02	Han-Uul	3.21316	1.27	55.49 ± 1.49	80.32	1.2412E-10
2014BA-23	Bayantsagaan	3.53169	1.13	90.55 ± 1.93	88.93	1.8198E-10

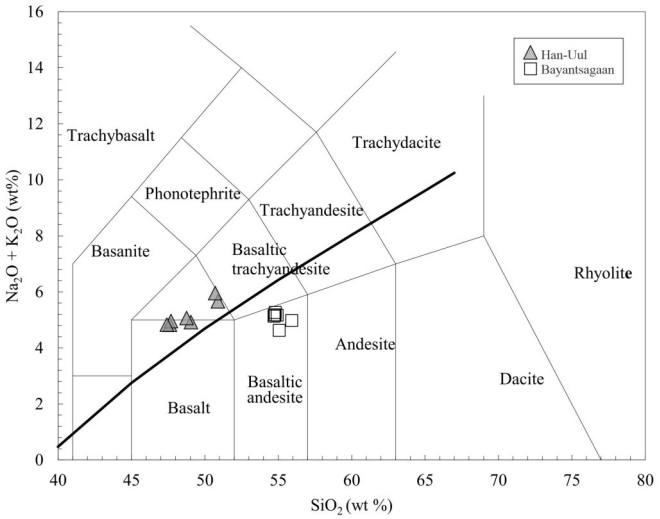

Fig. 4. Total alkalis (Na_2O+K_2O) versus SiO_2 (Le Bas et al., 1986) plot for analyzed samples from the Bayantsagaan and Han-Uul areas. Boundary line for alkaline and subalkaline series in figure (a) is from Irvine and Baragar (1971).

slightly higher $Fe_2O_3^t$ (10.42-11.35 wt%), TiO_2 (1.95-2.12 wt%), CaO (9-10.45 wt%), K_2O (1.42-2.01 wt%) than those from Bayantsagaan $Fe_2O_3^t$ (8.59-11.03 wt%), TiO_2 (1.39-1.81 wt%), CaO (6.47-8.07 wt%), K_2O (0.32-1.11). The Bayantsagaan basalts show higher SiO_2 (54.71-55.92 wt%), Al_2O_3 (15.0-18.43 wt%) contents than Han-Uul basalts (SiO_2 of 47.40-50.89; Al_2O_3 of 14.48-14.95 wt%). The Ni concentrations are variable.

In MgO variation diagrams (Fig. 5), the Han-Uul samples show weak negative correlation of SiO_2, TiO_2, and slightly positive correlation of Cr, Ni and $Fe_2O_3^T$, no correlation of CaO and CaO/Al_2O_3, with MgO. In contrast, Bayantsagaan basalts show no correlations of these oxides and trace elements with MgO.

All samples from Han-Uul and Bayantsagaan volcanic fields display similar chondrite-normalized REE and primitive mantle (PM-) normalized trace elements patterns (Fig. 6a, b) that resemble those of OIBs. In details, REE patterns characterized by sub parallel smooth curves from La to Lu displaying steep slopes with absence of Eu anomaly, indicating a significant enrichment of light rare earth elements (LREEs) relative to heavy rare earth elements (HREEs) (Fig. 6c, d). The degree of fractionation between LREE and HREE for the Han-Uul samples, with $(La/Yb)_N$ ratios of 9.25-11.38, was relatively higher than those of the Bayantsagaan samples with $La/Yb)_N$ ratios of 5.61-8.51. In primitive mantle normalized trace element diagrams, trace elements pattern exhibit distinct enrichment large ion lithophile elements (LILE; e.g. Rb, K, Sr, U), negative Ti and Y anomalies. Other distinctive features are noted that no depletion Nb, Ta exists in samples from Han-Uul in East Mongolia, whereas those from the Bayantsagaan show negative Nb and Ta anomaly.

Whole-rock Sr-Nd isotope

Sr –Nd isotopic compositions results of basalts are listed in Table 3. These results, together with published data for the late Mesozoic-Cenozoic basalts from Mongolia are plotted in Fig.7. $^{87}Sr/^{86}Sr$ and $^{143}Nd/^{144}Nd$ isotopic ratios for the Han-Uul basalts range from 0.704240 to 0.704546 and from 0.512903 to 0.513092, respectively, plotting within the field of OIB. The Bayantsagaan basalt has a relatively low $^{87}Sr/^{86}Sr$ ratio from 0.704691 to 0.704992 and relatively high $^{143}Nd/^{144}Nd$ value of 0.512709 to 0.512722, which are similar to those published previously (Yarmolyuk et al., 2015) and plots in the OIB field.

Table 2. Major (wt.%) and trace elements (ppm) compositions for late Cretaceous-early Cenozoic volcanic rocks from South

Locality	Bayantsagaan							Han-Uul						
Sample No	BA-01	BA-03	BA-16	BA-18	BA-19	BA-20	BA-22	UG-01	UG-03	UG-07	UG-08	UG-12	UG-14	UG-06
Rock type	**BA**	**BA**	**BA**	**BA**	**BA**	**BA**	**BA**	**B**	**B**	**B**	**B**	**TB**	**TB**	**B**
Oxides (wt. %)														
SiO_2	55.06	55.92	54.91	54.80	54.71	54.78	54.74	47.62	47.69	49.04	48.75	50.89	50.69	47.40
TiO_2	1.41	1.81	1.42	1.40	1.39	1.40	1.41	2.02	2.03	2.04	2.02	2.09	2.13	1.95
Al_2O_3	18.43	15.00	16.86	16.79	16.70	16.67	16.76	14.68	14.69	14.95	14.86	14.93	14.82	14.48
$Fe_2O_3^T$	8.59	11.03	9.48	9.51	9.72	9.64	9.62	11.33	11.40	11.35	11.30	10.46	10.42	11.08
MnO	0.18	0.19	0.13	0.13	0.13	0.13	0.13	0.16	0.16	0.16	0.16	0.13	0.13	0.16
MgO	3.36	4.25	4.54	4.71	4.86	4.81	4.74	9.90	9.51	7.46	7.65	6.11	6.27	9.24
CaO	8.07	6.47	7.11	7.03	6.98	7.02	7.06	9.00	9.10	9.65	9.77	9.28	9.11	10.45
Na_2O	4.30	4.45	4.06	4.09	4.27	4.13	4.09	3.31	3.45	3.50	3.62	3.90	3.95	3.41
K_2O	0.32	0.53	1.11	1.17	0.85	1.04	1.09	1.51	1.50	1.42	1.44	1.76	2.01	1.42
P_2O_5	0.27	0.35	0.37	0.38	0.37	0.37	0.38	0.46	0.47	0.42	0.42	0.45	0.47	0.40
TOTAL	100	100	100	100	100	100	100	100	100	100	100	100	100	100
LOI	1.78	0.80	1.42	1.08	0.70	1.06	1.14	1.54	2.06	1.26	1.36	1.64	1.44	1.36
Mg#	48	47	53	54	54	54	53	67	66	61	61	58	58	66
$Na_2O + K_2O$	4.62	4.98	5.17	5.26	5.13	5.17	5.17	4.82	4.96	4.92	5.07	5.66	5.95	4.83
K_2O/Na_2O	0.07	0.12	0.27	0.29	0.20	0.25	0.27	0.46	0.43	0.41	0.40	0.45	0.51	0.42
Trace elements (ppm)														
Sc	15.61	20.38	13.00	11.53	14.83	14.59	11.02	21.69	20.12	20.24	18.23	15.36	15.11	23.74
Ti	0.84	1.08	0.84	0.84	0.83	0.83	0.84	1.21	1.21	1.22	1.20	1.25	1.27	1.16
V	153	206	165	164	163	109	160	194	193	174	171	149	130	202
Cr	80	101	95	93	98	101	88	300	299	218	216	170	153	358
Co	27.7	23.6	28.6	28.6	29.1	29.6	27.3	45.5	45.7	39.4	40.6	37.9	30.8	45.0
Ni	102	64	265	210	142	108	132	246	261	227	224	184	140	240
Zn	102	121	103	103	108	109	100	102	103	94	98	107	92	104
Rb	4.9	7.6	19.7	19.0	15.7	19.2	19.2	29.3	28.2	23.7	24.6	32.7	33.7	26.4
Sr	599	455	623	600	632	603	600	579	576	520	510	553	572	639
Y	15.9	21.0	19.6	18.2	19.5	18.9	18.4	20.1	20.1	19.1	19.0	17.3	17.7	19.8
Zr	99	131	145	142	151	143	140	185	186	157	157	164	143	177
Nb	6.6	8.6	11.8	11.8	12.3	11.8	11.72	37.3	37.6	30.5	31.9	32.7	28.3	34.7
Cs	0.45	0.69	0.51	0.51	0.69	0.53	0.52	0.37	0.37	0.26	0.29	0.32	0.30	0.56
Ba	179	272	350	330	333	336	325	388	379	412	369	374	383	359
La	11.8	15.8	20.2	19.6	21.1	20.6	19.87	26.9	26.6	21.0	21.1	19.2	20.0	24.6
Ce	25.1	34.5	43.3	42.4	44.3	43.0	42.77	52.4	51.9	39.8	42.2	39.4	34.8	48.8
Pr	3.58	4.82	5.63	5.58	5.86	5.68	5.59	6.62	6.54	5.38	5.48	5.18	5.47	6.13
Nd	15.6	21.4	23.4	22.4	25.2	23.0	22.65	26.2	26.4	21.4	22.2	21.8	24.5	26.0
Sm	4.01	5.39	5.44	5.29	5.36	5.37	5.36	6.24	6.18	5.24	5.37	5.61	5.88	5.51
Eu	1.29	1.67	1.65	1.59	1.60	1.61	1.60	1.90	1.93	1.72	1.73	1.87	1.89	1.75
Gd	3.77	5.08	4.93	4.70	4.63	4.85	4.74	5.73	5.76	5.03	5.09	5.22	5.35	4.96
Tb	0.58	0.79	0.73	0.70	0.73	0.73	0.72	0.86	0.86	0.76	0.77	0.78	0.79	0.80
Dy	3.29	4.44	3.88	3.81	4.03	3.88	3.85	4.49	4.54	4.10	4.12	3.93	4.06	4.39
Ho	0.66	0.88	0.74	0.75	0.78	0.75	0.73	0.85	0.84	0.78	0.79	0.73	0.73	0.85

*B, basanite; BA, basaltic andesite; TB, trachy basalt.

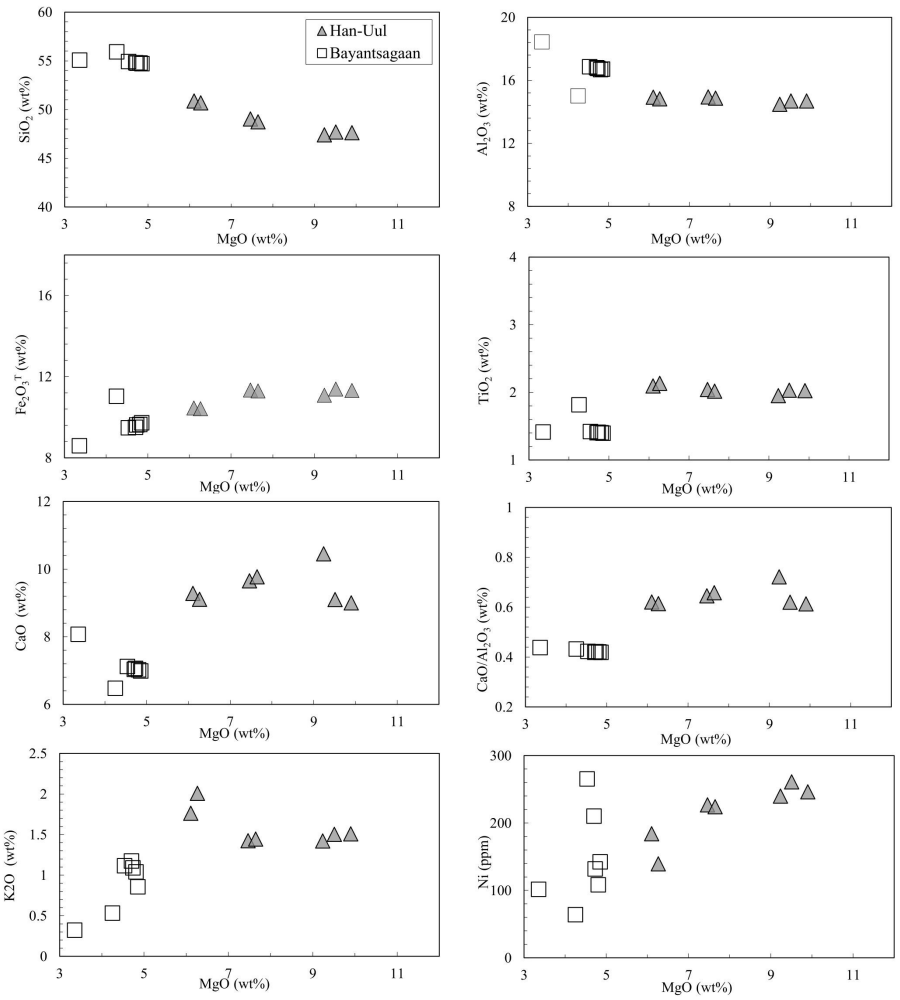

Fig. 5. Oxides, CaO/Al_2O_3, and trace elements Ni versus MgO plots for the basalts from the Bayantsagaan and Han-Uul volcanic provinces from the Bayantsagaan and Han-Uul volcanic provinces

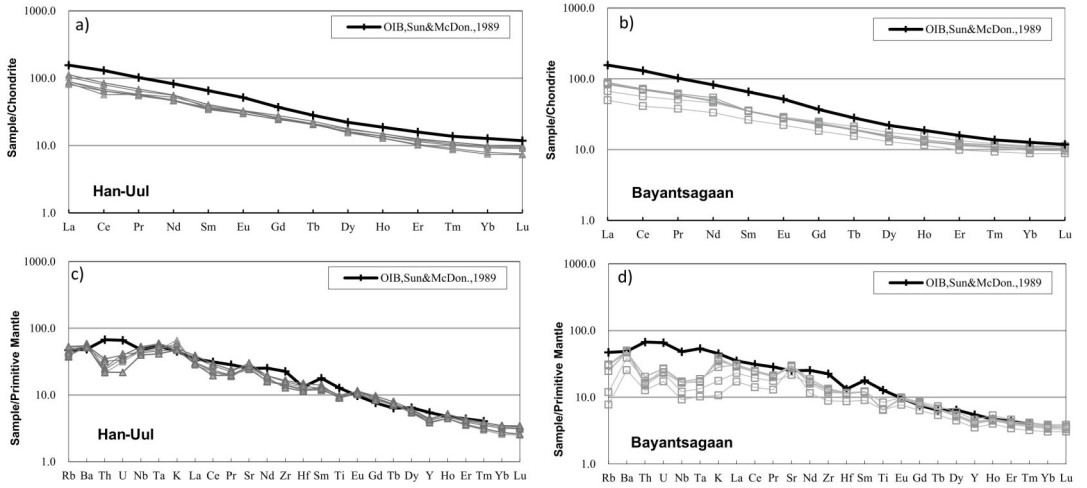

Fig. 6. Chondrite-normalized REE patterns and primitive mantle-normalized diagram for rocks of Early Cenozoic basalts from Han-Uul (a, c) late Cretaceous basalts from the Bayantsagaan (b, d) Normalizing values are from Sun and McDonough (1989) both chondrite and primitive mantle. For comparison, the ocean island basalt (OIB) (Sun and McDonough, 1989) is also plotted.

Table 3. Sr-Nd isotopes results of the late Cretaceous-early Cenozoic volcanic rocks

Sample No	BA-22	BA-03	UG-01	UG-14
Rock type	BA	BA	B	B
Rb[μg/g]	20.1	8.2	31.3	36.6
Sr[μg/g]	627	483	622	622
$^{87}Rb/^{86}Sr$	0.0928	0.0491	0.145	0.175
$^{87}Sr/^{86}Sr$	0.704992	0.704691	0.704240	0.704546
Error	0.00001	0.000011	0.000012	0.000011
Sm[μg/g]	5.14	5.43	6.0	5.6
Nd[μg/g]	23.1	21.7	26.5	23.5
$^{147}Sm/^{144}Nd$	0.1345	0.154	0.1359	0.1440
$^{143}Nd/^{144}Nd$	0.512722	0.512709	0.512903	0.513092
Error	0.000005	0.000009	0.000008	0.000012
$e_{Nd}(t)$	2.40	2.00	5.17	8.86

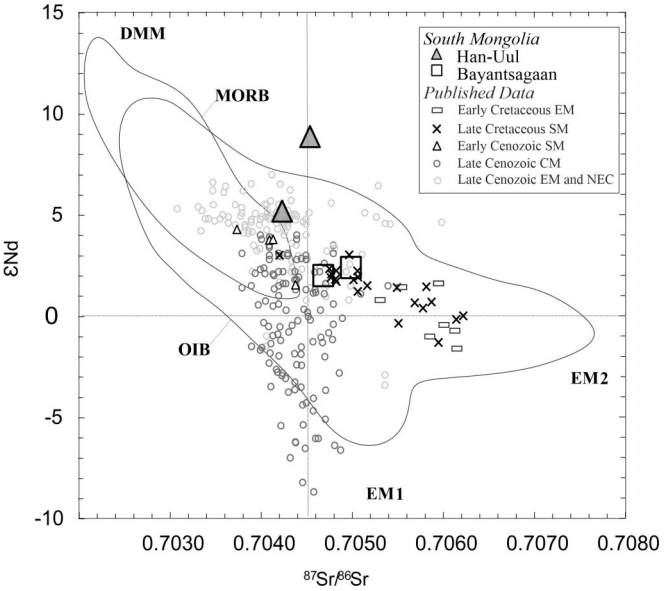

Fig. 7. $^{143}Nd/^{144}Nd$ versus $^{87}Sr/^{86}Sr$ plot for the late Cretaceous-early Cenozoic basalts from South Mongolia. Previously published Sr-Nd isotopic data for the late Mesozoic-Cenozoic basalts are also plotted for comparison. Data sources are Rasskazov et al. (2002), Yarmolyuk et al. (2003), Barry et al. (2003), Togtokh et al. (2018), Xu and Zheng (2017). Reference fields for DM (depleted mantle), EM1 and EM2 (enriched mantle), MORB (mid-ocean range basalt) and OIB (oceanic island basalt) are from Stracke et al. (2003, 2005). Abbreviation CM-Central Mongolia, NEC-North East China, SM-South Mongolia

DISCUSSION

The late Cretaceous-early Cenozoic volcanic rocks in South Mongolia essentially have similar geochemical features although there are some variations in elements content. These similarities and variations might be due to mixture of factors, including post-magma alteration, crustal contamination, fractional crystallization, mantle source, and partial melting degree. Therefore, the effects of these parameters should be evaluated before the data can be used for constraining natures of the magma source.

Influence of post-magmatic alteration

The LOI (loss on ignition) value of a whole-rock analysis is an indicator for presence of secondary alteration or hydrous-bearing minerals. All studied samples show low LOI contents (-0.70-1.78) suggest that post-magmatic alteration has little influence on those volcanic rocks. Alternative, the influence of alteration on the major elements can also be evaluated by applying the Chemical Index of Alteration [$CIA=Al_2O_3/(Al_2O_3+CaO+Na_2O+K_2O)$] (Nesbitt and Young, 1982). The degree of influence of alteration can be divided into four levels: no influence (fresh rock), slightly altered rocks, moderately altered rocks and strongly altered rocks, which have CIA values of <50, 50-65, 65-85, and >85, respectively. The CIA values of the samples range from 57 to 59 for the Bayantsagaan and 49 to 52 for the Han-Uul. These suggest that the alteration has just negligible effect on the composition of the volcanic rocks in this study.

Fractional crystallization

The Bayantsagaan samples have low MgO contents (mostly <8 wt%) and Mg# (47-67). They are far from those of expected melts in equilibrium with mantle peridotites (Frey et al., 1978; Cox, 1980). Major oxides, and compatible elements (Ni and Cr) are not linerily correlated with MgO contents (Fig. 5). These signatures suggest that Bayantsagaan basalts did not experience sigificant fractional crystallization of olivine and pyroxene. Similarly, absence of Eu anomaly demonstrates fractional crystallization of plagioclase did not occurred for the Bayantsagaan basalts. Han-Uul basalts have variable MgO contents (6.3-9.9 wt%) and Mg# (58-67). SiO_2 and Al_2O_3 contents increase and Ni decreases with MgO decrease (Fig. 5), apparently indicating fractional crystallization

of olivine. Both CaO and CaO/Al_2O_3 does not correlate with MgO, implying clinopyroxene fractionation is insignificant. Plagioclase appears to be common in the basaltic rocks from these two fields, but absence of both negative Eu anomaly and no positive Al_2O_3–MgO trend excludes the possibility of plagioclase fractionation (Fig. 5).

Additionally, all the basalts show distinct negative Ti anomaly in the PM-normalized trace element diagram regardless of TiO_2 contents and the volcanic provinces (Fig. 6c, d). However, there is no positive correlation between TiO_2 and MgO, indicating that fractional crystallization of Ti-oxide minerals can be ruled out. As a result, we conclude that the role of fractional crystallization is insignificant in the genesis of the basalts in both late Cretaceous and early Cenozoic in South Mongolia.

Crustal contamination

Continental basalts maybe more likely affected by crystal contamination than basalts formed in oceans (e.g. MORB and OIB) because the continental basaltic magma has to pass through the thick continental crust to the surface.

Ba/Nb and La/Nb ratios of the Han-Uul samples overlap with global OIB and nearly show no crustal contamination, whereas samples from Bayantsagaan display the positive correlation between Ba/Nb and La/Nb plotting along the expected contamination trend (Fig. 8a). However, if continental crust were involved in petrogenesis of the Bayantsagaan volcanism, the most contaminated sample with the lowest εNd would also display the lowest Sm/Nd (Xu et al., 2005). Such positive correlation cannot be observed in the Bayantsagaan, even in the

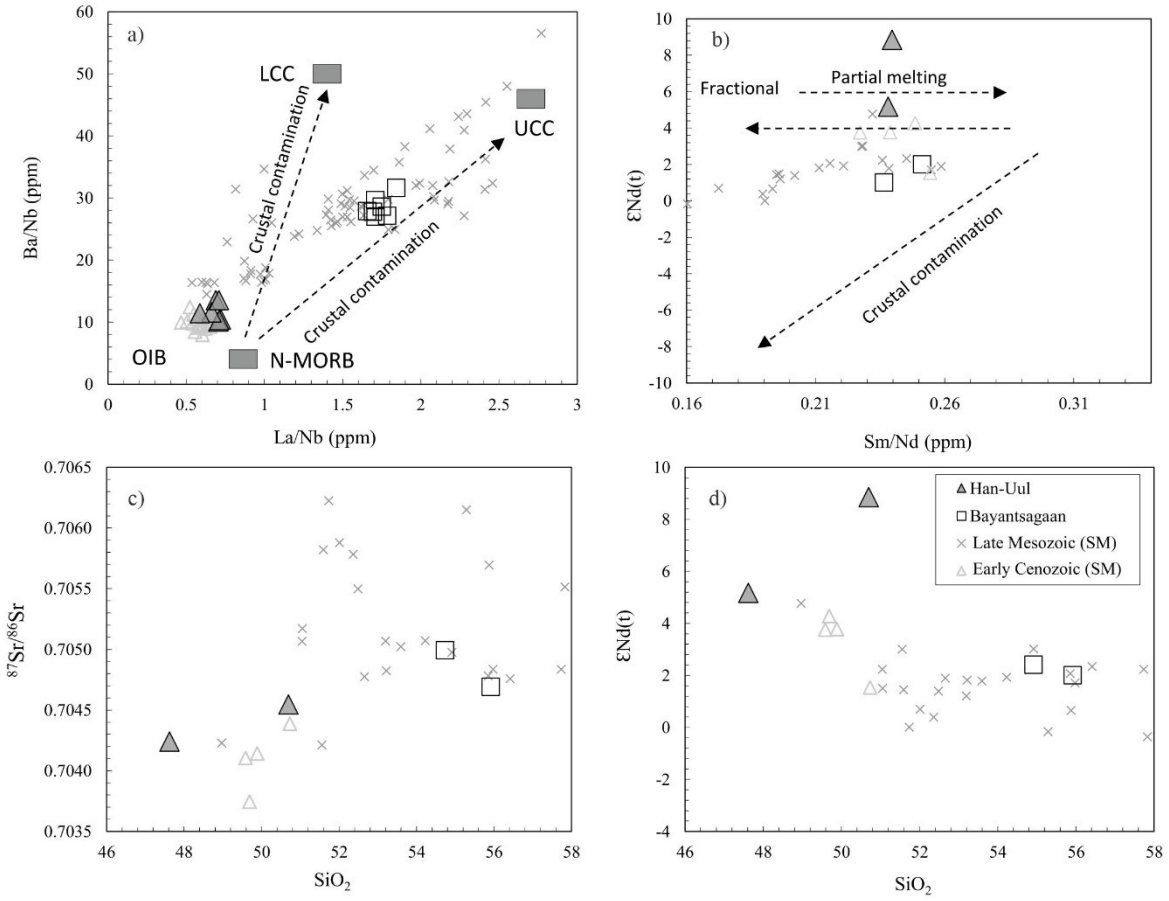

Fig. 8. Diagrams of La/Nb versus Ba/Nb (a), εNd(t) versus Sm/Nd (b), $^{87}Sr/^{86}Sr$ versus SiO_2 (c), εNd(t) versus SiO_2 (d) for all analyzed basaltic samples from Bayantsagaan and Han-Uul. Previously published Sr-Nd isotopic data (cross) taken from Barry et al. (2003), Yarmolyuk et al. (2015)

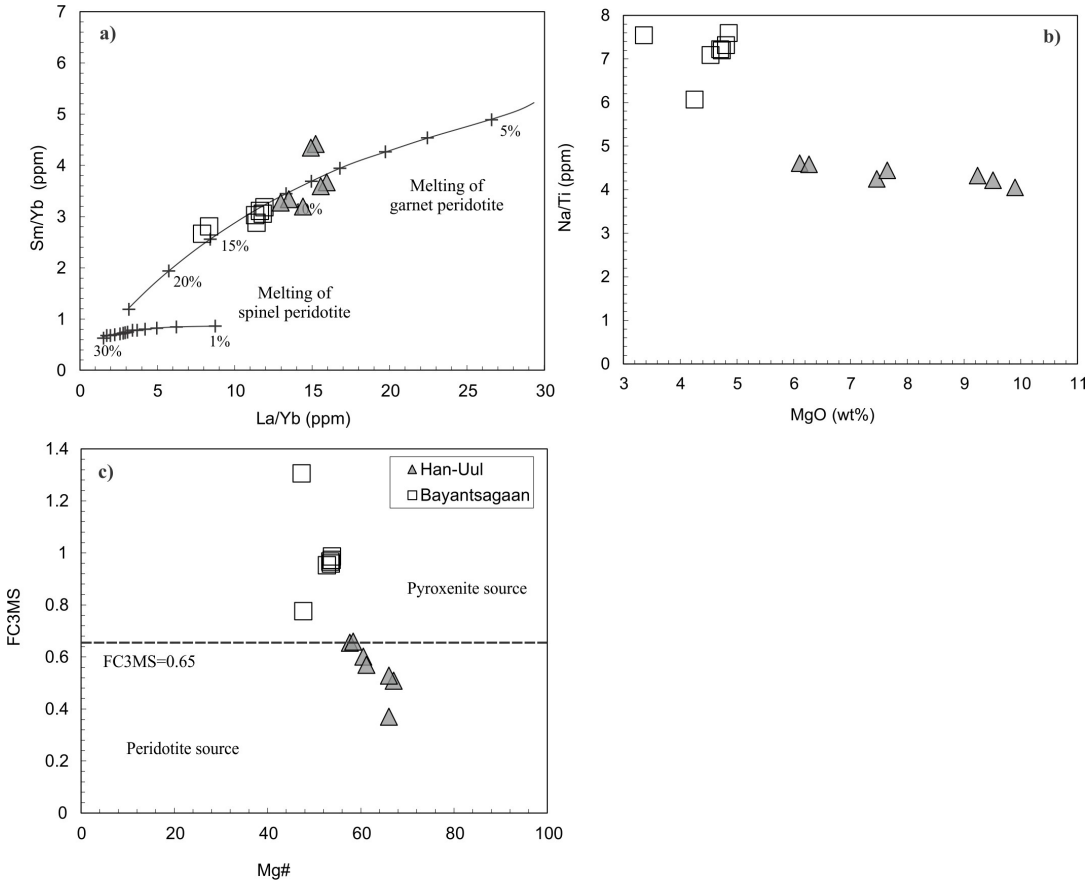

Fig. 9. Diagram of La/Yb versus Sm/Yb (a) Na/Ti cation fraction ratios with MgO (b) FC3MS versus Mg# (c) for all analysed basaltic samples from Bayantsagaan and Han-Uul. Batch melting curves calculated for garnet peridodite. Partition coefficients are taken from Putirka (1999b).

Han-Uul field. Instead they show flat εNd(t)-Sm/Nd trend related with fractional crystallization and/or partial melting processes (Fig. 8b). Moreover, as shown in Fig. 8c, d, $^{87}Sr/^{86}Sr$ remain nearly constant with increasing SiO_2, differing from effects of significant crustal contamination.

Therefore, geochemical data suggest that the role of crustal contamination could be negligible in the petrogenesis of the basalts from Bayantsagaan and Han-Uul. Although Bayantsagaan basalts maybe affected by crustal contamination, to the effect have been limited and has not significantly altered the elemental concentrations and isotopic ratios of the erupted magmas. Crustal assimilation coupled with fractional crystallization (AFC) is also unlikely because no progressive decreases in Cr, Ni, Co and Mg# with concomitant increase in $^{87}Sr/^{86}Sr$ ratios and decrease in $^{143}Nd/^{144}Nd$ ratios are observed.

Partial melting and mantle source

The characteristics of the mantle sources can be distinguished by plotting La/Yb against Sm/Yb. Since Yb is compatible in garnet whereas La and Sm are incompatible. Therefore La/Yb and Sm/Yb will be strongly fractionated when melting degree is low if there are garnets in the mantle source; La/Yb is only weakly fractionated and Sm/Yb is nearly unfractionated during the melting in the spinel stability field. In the Sm/Yb vs. La/Yb diagram (Fig. 9a), it is evident that variable degrees (9–15%) of batch melting of a hypothetical light REE-enriched mantle source ($[La/Yb]_N > 1$) in the garnet stability field can generate the La/Yb–Sm/Yb systematics of the basalts studied. Specifically, the Han-Uul basalts have a lower degree of melting (9–10%) than the Bayantsagaan (11–15%) and indicative of residual garnet in the source region. The Bayantsagaan rocks, which are not strongly HREE depleted, are presumed

to have little interaction with garnet. Since the melting degree is inversely proportional to melting pressure/depth (Langmuir et al., 1992), it can be inferred that the Han-Uul basalts may have been generated at a deeper depth than Bayantsagaan volcanic rocks.

The ratio of Na/Ti (cation) is sensitive to the pressure of melts segregation (Putirka, 1999a), and it can be used to evaluated the melting depth/pressure. Na/Ti of melts decreases with increasing mean pressure, because the clinopyroxene-melt partition coefficient of Na increases with increasing pressure (Blundy et al., 1995; Kinzler, 1997), while both the clinopyroxene- and garnet-melt partition coefficients of Ti remain constant or decrease (Kinzler, 1997; Putirka, 1999a). Na/Ti ratio of the Bayantsagaan basalts is the high (Fig. 9b), ranging from 6.06 to 7.21. The Han-Uul basalts have low Na/Ti values (ranging from 4.04-4.58). These demonstrate that the Bayantsagaan basalts maybe formed at the shallower depth whereas Han-Uul basalts formed at the deeper depth. This conclusion is in accordance with that constrained from the La/Yb–Sm/Yb systematics of the basalts, as abovementioned.

Peridotite has been widely accepted to be the mantle source of OIB and MORB; however, diverse magma sources including pyroxenite, hornblendite, and carbonated peridotite, are also proposed (e.g., Kogiso and Hirschmann, 2006). Whole-rock compositions can be used to investigate the lithology of mantle sources of basalts. According to the parameter FC3MS, which is defined as $FeO^T/CaO-3MgO/SiO_2$, with FC3MS value of 0.65 as the boundary between pyroxentie and peridotite sources (Yan and Zhao, 2008), the mantle source of the basalts in Han-Uul is dominated by peridotite, whereas the sources of the basalts in Bayantsagaan is likely the mixing of peridotite-pyroxenite (Fig. 9c).

Moreover, the PM-normalized trace element distribution patterns of the basalts in this study display positive anomalies at Ba, K and Sr (Fig. 5), suggesting that hydrous phases, such as amphibole and phlogopite, exist in the mantle sources (Ba from phlogopite and Sr from amphibolite). This suggests that the mantle sources of the basalts in two fields were metasomatized before their eruption. It is needed to point out that Nb is highly compatible in Ti-oxide minerals (e.g. rutile), and the complete consumption of Ti-oxide minerals during partial melting of the sources will cause positive Nb anomaly, but the negative Ti anomaly of Han-Uul basalts (Fig. 6) attests that the Nb enrichment would be mainly caused by the hydrous phases (e.g. amphibole).

Magma genesis

Numerous studies have suggested that the Mesozoic-Cenozoic continental basalts in NE Asia including Mongolia were formed by partial melting of mantle sources characterized by mixing of DM and EM1, resembling the OIBs (e.g., Barry and Kent, 1998, 2003; Hunt et al., 2012; Yarmolyuk et al., 2015; Xu et al., 2005; Xu and Zheng, 2017 more).

Late Cretaceous Bayantsagaan volcanic rocks show high $^{87}Sr/^{86}Sr$ and low $^{143}Nd/^{144}Nd$, and are depleted in HFSEs. Combining the published Sr-Nd isotope data point to slightly depleted and PM-like mantle source (Fig. 7) which is likely to be lithospheric mantle of CAOB (Zhang et al., 2007; Zhou et al., 2009). Therefore, metasomatized lithospheric mantle will account for the genesis of the late Cretaceous basalts in South Mongolia. Compared with the late Mesozoic volcanism in East Mongolia which is characterized by the co -existence of mafic and silicic magmas, like bimodal series (Dash et al., 2013, Bars et al., 2018) suggest negative eNd(t) and might have been derived from the metasomatized lithospheric mantle which incorporated significant amount of continental crust components.

Whereas Early Cenozoic basalts in South Mongolia display a depleted isotopic composition without HFSE anomalies. The Han-Uul basalts are characterized by relatively high $^{87}Sr/^{86}Sr$ and $^{143}Nd/^{144}Nd$, with the latter close to that of N-MORB. These suggest that the early Cenozoic basalts originated from an asthenospheric mantle source that might have been metasomatized by an agent that is relatively high in $^{143}Nd/^{144}Nd$. Besides, the late Cenozoic Central-Northern Mongolia basalts

show some Sr-Nd isotope differences from the DM-EMI mixing trend for the typical OIB (Fig. 7), and these basalts can be explained by asthenosphere-derived melt reacts with the metasomatized SCLM, or mix melts originating from the SCLM (Barry et al., 2007, Togtokh et al., 2018).

Geodynamic implications

It is commonly accepted that the Late Mesozoic volcanic rocks in Mongolia and NE China were formed in an extensional environment (e.g., Faure and Natal'in, 1992).

Back arc extension model related to the subduction and stagnant of the Pacific Plate in East Asia continent has been widely accepted for explaining the geodynamic setting of the late Mesozoic volcanic rocks in eastern North East Asia (e.g., Sun et al., 2013; Zhang et al., 2011). As a matter of fact, the Late Mesozoic volcanic rocks in South and East Mongolia, and NE China are discontinuously distributed, and individual volcanic belts generally extend in a NNE direction, parallel to the Mesozoic volcanic sedimentary basins (e.g., the Hailar and the Song Liao basins), both of which are conformable to the Pacific subduction zone (e.g., Li, 2000; Wu et al., 2005) which all implies that the volcanism is likely related to the Pacific subduction. Therefore, we prefer the model of the back-arc extension induced by the westward Pacific-subduction, as suggested by Bars et al. (2018) to interpret the geodynamic settings Late Cretaceous volcanic rocks in

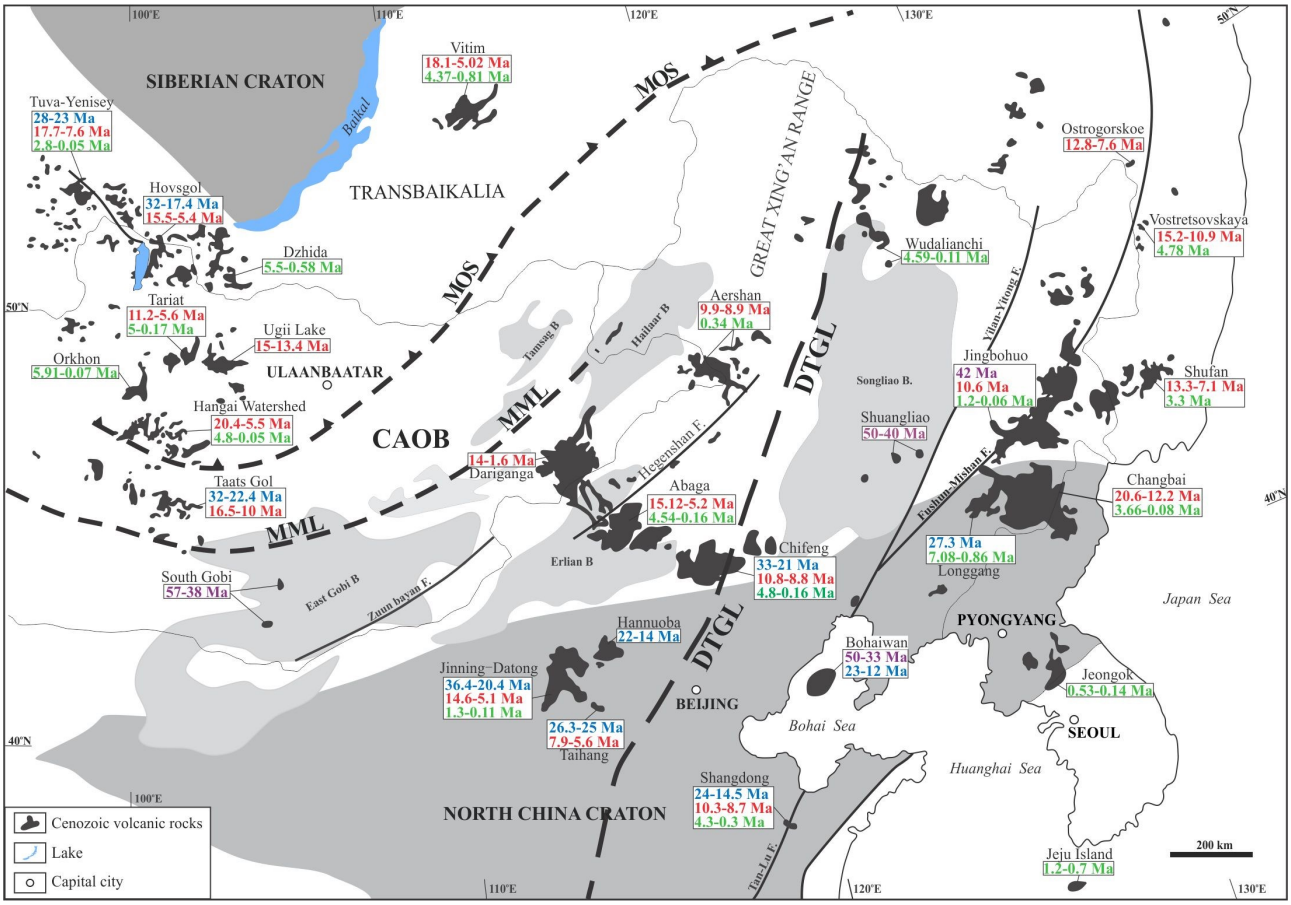

Fig. 10. Simplified map showing the temporal-spatial distribution of the Cenozoic OIB-like volcanic rocks in NE Asia. The numbers in brown, blue, red, and green colors in rectangles denote available K-Ar or Ar-Ar ages of the volcanic rocks that are approximately between 60-40, 35-20, 15-5, and <5 Ma, respectively. MOS: Mongol-Okhotsk suture; MML: Main Mongolian Lineation; DTGL: Daxing'anling-Taihangshang gravity lineation; CAOB: central Asian orogenic belt. Data sources are from Höck et al. (1997), Liu et al. (2001), Devyatkin (2002), Tang et al. (2006), Chashchin et al. (2007), Ryu et al. (2011), Xu et al. (2012), Ivanov et al. (2015), and Yarmolyuk et al. (2015).

South Mongolia. Model emphasizes that the slab rollback of the subduction retreat of the Pacific Plate might have caused the upwelling of the asthenosphere, which in turn caused the extension and melting of the overriding lithospheric mantle, to generate the Late Mesozoic volcanic rocks.

Mantle plume has long been advocated to interpret the geodynamic setting of the Cenozoic volcanic rocks in Mongolia (e.g., Khain, 1990; Windley and Allen, 1993; Cunningham, 1998; Mordvinova et al., 2007), but recent studies do not support this suggestion (e.g., Barry et al., 2003, 2007), which show only localized upper mantle anomalies in Mongolia.

The BMW (Big Mantle Wedge) model related to the subduction and stagnant of the Pacific Plate in East Asia continent explain the geodynamic setting of the Cenozoic basalts in eastern North East Asia (e.g., Huang and Zhao, 2006; Zhao et al., 2009; Xu, 2014; Xu and Zheng, 2017 and references therein). On the contrary, some authors argued that the Indo-Asian collision or the collision coupling with the Pacific subduction would account for the

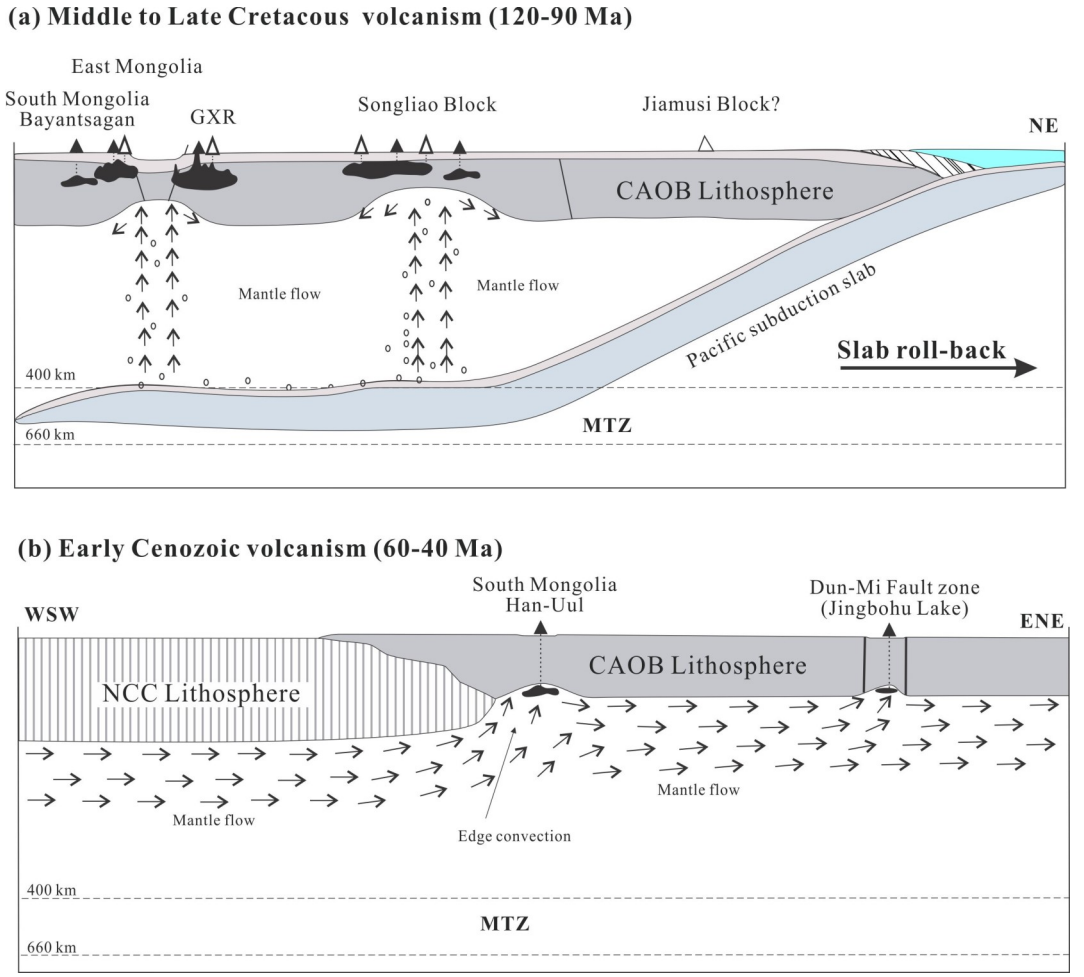

Fig. 11. Cartoon diagrams showing the possible petrogenesis and geodynamic settings in which the South Mongolian late Mesozoic-early Cenozoic basalt generated. (a) The model of back-arc extension, possibly induced by slab rollback of the westward subducted Pacific Plate and the subduction zone retreat, can explain the geodynamic setting of the Late Mesozoic volcanism in South and East Mongolia.(b) An edge convection model to explain the formation of the late Cretaceous-early Cenozoic volcanic rocks (60-40 Ma) in South Mongolia mainly along the juxtaposed margins of the NCC and CAOB. Melts from decompression melting of a small-scale shallow mantle upwelling reacting with the overlying lithosphere to produce the Han-Uul volcanic rocks in South Mongolia. MOO: Mongol-Okhotsk Ocean; DTGL: Daxing'anling-Taihangshang gravity lineation; CAOB: Central Asian Orogenic Belt; GXR-Great Xing'an Range.

geodynamic setting of the Cenozoic rifting and volcanism in eastern China. Considering that the -early Cenozoic volcanism is coeval with, or slightly later than, the Indo-Asian collision, we use the "edge convection model" (King and Anderson, 1998) to explain the generation of the early Cenozoic volcanism. The edge convection model predicts that decompression melting of the asthenosphere or lithosphere occurs at juxtaposed margins of thick-to-thin lithosphere, where rapid shallowing of the asthenospheric mantle enables melting. As such, the decompression melts from the upwelling asthenosphere was underplated at the bottom of the lithosphere and reacted with the overlying lithosphere to form the observed basalts showing Sr-Nd isotopic signature of involvement of the lithosphere. Alternatively, the excess heat from the upwelling asthenosphere itself and/or from the asthenosphere-derived melts can cause partial melting of the lowermost lithosphere and these lithosphere-derived melts may be mixed with the asthenosphere-derived melts to produce the basalts. Obviously, the contrasting lithosphere thickness of the NCC and the CAOB favors a formation of edge convection. Additionally, the spatial and temporal distribution of the OIB-like Early Cenozoic volcanism in NE Asia occur mainly in the conjunction of the ancient cratons. Fig 10.

Therefore, we propose that the generation of the early Cenozoic volcanism in Mongolia is probably related to the shallow mantle upwelling induced by the edge convection along the northern margin of the NCC during or following the Indo-Asian collision (e.g., Rowley, 1996; Zhu et al., 2005; Zhang et al., 2012) and might have reinforced the far-field effect of the Indo-Asian collision or the collision-driven mantle flow as suggested by Liu et al. (2004) but influence of the far-field effect of the Pacific subduction cannot be completely excluded. It is worthy to note that the mantle upwelling induced by the edge convection is probably small in size and thus easily shrinks or disappears with time. This is likely the reason that no low-V anomalies (Liu et al., 2004) presently exist under some regions where the early Cenozoic volcanism occur.

To sum up, from the discussion above, we illustrate the geodynamic setting and processes that probably operated in the generation of the late Cretaceous and early Cenozoic basalts in South Mongolia, in Fig. 11.

CONCLUSIONS

(1) The Mesozoic volcanism in South Mongolia was formed during nearly late Cretaceous (110-90) Ma time, whereas Cenozoic volcanic activity erupted during 55-40 Ma in South Mongolia.

(2) The late Cretaceous-early Cenozoic basalts in South Mongolia are predominantly alkaline and tholeiitic. They show similar geochemical feature of typical OIB, although they somewhat varied with time. The compositions systematically evolved with a gradual increase in the content of HFSE (Nb and Ta) in younger rocks. These basalts experienced insignificant crustal contamination and crystal fractionation.

(3) Both mantle source and melting conditions contribute to the compositional variations of these OIB-like basalts. Late Cretaceous basalts were likely formed by higher degree melting of garnet facies mantle with higher proportion pyroxenite, whereas early Cenozoic volcanic rocks in south Mongolia were likely derived from lower degree melting of peridotite.

(4) Late Cretaceous basalts from the South Mongolia have high $^{87}Sr/^{86}Sr$ and low $^{143}Nd/^{144}Nd$ showing mixing trend of the depleted (DM) and enriched mantle (EM), whereas Cenozoic basalts display a depleted mantle isotopic composition.

(5) Late Cretaceous volcanic rocks (114-90 Ma) might have related back arc-extension possibly induced by slab rollback of the westward subducted Pacific Plate and the subduction zone retreat. Whereas the early Cenozoic volcanism (60-40 Ma), which mainly occur along the conjunction of the NCC and CAOB, is probably related to mantle upwelling induced by edge convection during or following the Indo-Asian collision.

ACKNOWLEDGMENTS

This study is supported by the National Key R&D Program of China (Grant No.: 2017YFC0601306), the National Natural Science Foundation of China (Grant No.: 41273071), the Ministry of Science and Technology of China (Grant 2012FY120100) and the Chinese Academy of Sciences-Third World Academy of Sciences (CAS-TWAS) President's PhD Fellowship Program.

REFERENCES

Barry, T.L. 1999. Origins of Cenozoic basalts in Mongolia: a chemical and isotope study. PhD thesis, University of Leicester, 263 p.

Barry, T.L., Ivanov, A.V., Rasskazov, S.V., Demonterova, E.I., Dunai, T.J., Davies, G.R., Harrison, D. 2007. Helium isotopes provide no evidence for deep mantle involvement in widespread Cenozoic volcanism across Central Asia. Lithos 95, 415-424. https://doi.org/10.1016/j.lithos.2006.09.003

Barry, T.L., Kent, R.W. 1998. Cenozoic magmatism in Mongolia and the origin of central and east Asian basalts. In: Flower, M., Chung, S.-L., Lo, C,-H., Lee, T.-Y. (eds) Mantle Dynamics and Plate Interactions in East Asia. American Geophysical Union Monograph, Geodynamics Series 27, 347-364. https://doi.org/10.1029/GD027p0347

Barry, T.L., Saunders, A.D., Kempton, P.D., Windley, B.F., Pringle, M.S., Dorjnamjaa, D., Saandar, S. 2003. Petrogenesis of Cenozoic basalts from Mongolia: evidence for the role of asthenospheric versus metasomatised lithospheric mantle sources. Journal of Petrology 44, 55-91. https://doi.org/10.1093/petrology/44.1.55

Bars, A., Miao, L., Fochin, Z., Munkhtsengel, B., Chimedtseren, A., Togtokh, K., 2018. Petrogenesis and tectonic implication of the Late Mesozoic volcanic rocks in East Mongolia. Geological Journal. https://doi.org/10.1002/gj.3080

Blundy, J.D., Falloon, T.J., Wood, B.J., Dalton, J.A. 1995. Sodium partitioning between clinopyroxene and silicate melts. Journal of Geophysical Research 100, 15501-15515. https://doi.org/10.1029/95JB00954

Chashchin, A.A., Martynov, Y.A., Rasskazov, S.V., Maksimov, S.O., Brandt, I.S., Saranina, E.V. 2007. Isotopic and geochemical characteristics of the late Miocene subalkali and alkali basalts of the southern part of the Russian Far East and the role of continental lithosphere in their genesis. Petrology 15, 575-598. https://doi.org/10.1134/S0869591107060045

Cox, K.G. 1980. A model for flood basalt volcanism. Journal of Petrology 21, 629-650. https://doi.org/10.1093/petrology/21.4.629

Cunningham, W.D. 1998. Lithospheric controls on late Cenozoic construction of the Mongolian Altai. Tectonics 17, 891-902. https://doi.org/10.1029/1998TC900001

Dash, B., Yin, A., Jiang, N., Tseveendorj, B., Han, B. 2013. Petrology, structural setting, timing, and geochemistry of Cretaceous volcanic rocks in eastern Mongolia: Constraints on their tectonic origin. Gondwana Research 27, 281-299. https://doi.org/10.1016/j.gr.2013.10.001

Devyatkin, E.V. 2004. Geochronology of Cenozoic basalts in Mongolia and their relationships with neotectonic structures. Stratigraphy and Geological Correlation 12, 199-209.

Devyatkin, E.V., Balogh, K., Dudich, A. 2002. Geochronology of basalts from the Valley of Lakes, Mongolia, and their correlation with the Cenozoic sedimentary sequence. Russian Journal of Earth Science 4, 389-397. https://doi.org/10.2205/2002ES000100

Enkhtuvshin, H., Savada, U., Eetaya, T., Eezumee, S. 1995. A petrological study on the Late Mesozoic and Cenozoic Volcanic Rocks of the Mongolian Plateau. Problems of Geology and Paleontology of Mongolia, 75-77.

Faure, M., Natal'in, B. 1992. The geodynamic evolution of the eastern Eurasian margin in Mesozoic times. Journal of Tectonophysics, 208, 397-411. https://doi.org/10.1016/0040-1951(92)90437-B

Frey, F.A., Green, D.H., Roy, S.D. 1978. Integrated models of basalt petrogenesis: A study of quartz tholeiites to olivine melilitites from South Eastern Australia utilizing geochemical and experimental petrological data. Petrology 19, 463-513. https://doi.org/10.1093/petrology/19.3.463

Guo, Z., Wilson, M., Liu, J., Mao, Q. 2006. Post-collisional, Potassic and Ultrapotassic Magmatism of the Northern Tibetan Plateau: Constraints on Characteristics of the Mantle Source, Geodynamic Setting and Uplift Mechanisms. Journal of Petrology 47, 1177-1220. https://doi.org/10.1093/petrology/egl007

Höck, V., Daxner-Höck, G., Schmid, H.P., Badamgarav, D., Frank, W., Furtmüller, G., Montag, O., Barsbold, R., Khand, Y., Sodov, J. 1997. Oligocene-Miocene sediments, fossils and basalts from the Valley of Lakes (Central Mongolia) - An integrated study. Mitteilungen der

Oesterreichischen Geologischen Gesellschaft, 90, 83-125.

Huang, J., Zhao, D. 2006. High-resolution mantle tomography of China and surrounding regions. Journal of Geophysical Research 111, https://doi.org/10.1029/2005JB004066

Hunt, A.C., Parkinson, I.J., Harris, N.B.W., Barry, T.L., Rogers, N.W., Yondon, M. 2012. Cenozoic volcanism on the Hangai dome, Central Mongolia: geochemical evidence for changing melt sources and implications for mechanisms of melting. Journal of Petrology 53, 1913-1942. https://doi.org/10.1093/petrology/egs038

Irvine, T.N., Baragar, W.R.A. 1971. A guide to the chemical classification of the common volcanic rocks. Canadian Journal of Earth Sciences 8, 523 -548. https://doi.org/10.1139/e71-055

Ivanov, A.V., Demonterova, E.I., He, H., Perepelov, A.B., Travin, A.V., Lebedev, V.A., 2015. Volcanism in the Baikal rift: 40 years of active-versus-passive model discussion. Earth-Science Reviews 148, 18-43. https://doi.org/10.1016/j.earscirev.2015.05.011

Jahn, B.-M., Capdevila, R., Liu, D., Badarch, G. 2004. Sources of Phanerozoic granitoids in the transect Bayanhongor-Ulaan Baatar, Mongolia: Geochemical and Nd isotopic evidence, and implications for Phanerozoic crustal growth. Journal of Asian Earth Sciences 23, 629-653. https://doi.org/10.1016/S1367-9120(03)00125-1

Khain, V.E. 1990. Origin of the Central Asian mountain belt: collision or mantle diaprism. Journal of Geodynamics 11, 389-394. https://doi.org/10.1016/0264-3707(90)90018-P

King, S., Anderson, D.L. 1998. Edge-driven convection. Earth and Planetary Science Letters 160, 289- 296. https://doi.org/10.1016/S0012-821X(98)00089-2

Kinzler, R.J. 1997. Melting of mantle peridotite at pressure approaching the spinel to garnet transition: application to mid-ocean ridge petrogenesis. Journal of Geophysical Research 102, 853- 874. https://doi.org/10.1029/96JB00988

Kogiso, T., Hirschmann, M.M. 2006. Partial melting experiments of bimineralic eclogite and the role of recycled mafic oceanic crust in the genesis of ocean island basalts. Earth and Planetary Science Letters 249, 188-199. https://doi.org/10.1016/j.epsl.2006.07.016

Kuritani, T., Ohtani, E., Kimura, J.-I. 2011. Intensive hydration of the mantle transition zone beneath China caused by ancient slab stagnation. Nature Geoscience 4, 713-716. https://doi.org/10.1038/ngeo1250

Langmuir, C.H., Klein, E.M., Plank, T. 1992. Petrological systematics of mid-ocean ridge basalts: constraints on melt generation beneath ocean ridges. In: Morgan, J.P., Blackman, D.K., Sinton, J.M. (Eds.) Mantle Flow and Melt Generation at Mid-Ocean Ridges. American Geophysical Union, Geophysics Monograph Series 71, 81-189.

Le Bas, M.J., LeMaitre, R.W., Streckeison, A., Zanettin, B. 1986. A chemical classification of volcanic rocks based on the total alkali-silica diagram. Journal of Petrology 27, 745-750. https://doi.org/10.1093/petrology/27.3.745

Li, C.-F., Li, X.-H., Li, Q.-L., Guo, J.-H., Li, X.-H., Feng, L.-J., Chu, Z.-Y. 2012a. Simultaneous determination of 143Nd/144Nd and 147Sm/144Nd ratios and Sm-Nd contents from the same filament loaded with purified Sm-Nd aliquot from geological samples by isotope dilution thermal ionization mass spectrometry. Analytical Chemistry 84, 6040-6047. https://doi.org/10.1021/ac300786xPMid:22746207

Li, X.H. 2000. Cretaceous magmatism and lithospheric extension in southeast China. Journal of Asian Earth Sciences, 18, 293-30. https://doi.org/10.1016/S1367-9120(99)00060-7

Liu, J., Han, J., Fyfe, W. 2001. Cenozoic episodic volcanism and continental rifting in northeast China and possible link to Japan Sea development as revealed from K-Ar geochronology. Tectonophysics 339, 385-401. https://doi.org/10.1016/S0040-1951(01)00132-9

Liu, M., Cui, X., Liu, F. 2004. Cenozoic rifting and volcanism in eastern China: a mantle dynamic link to the Indo-Asian collision? Tectonophysics 393, 29-42. https://doi.org/10.1016/j.tecto.2004.07.029

Miao, L., Fan, W., Liu, D., Zhang, F., Shi, Y., Guo, F. 2008. Geochronology and geochemistry of the Hegenshan ophiolitic complex: Implications for late-stage tectonic evolution of the Inner Mongolia-Daxinganling Orogenic Belt, China. Journal of Asian Earth Sciences 32, 348-370. https://doi.org/10.1016/j.jseaes.2007.11.005

Miao, L., Zhang, Fo., Baatar, M., Zhu, M., Anaad, Ch. 2017. SHRIMP zircon U-Pb ages and tectonic implications of igneous events in the Ereendavaa metamorphic terrane in NE Mongolia. Journal of Asian Earth Sciences, 144, 243-260. https://doi.org/10.1016/j.jseaes.2017.03.005

Mordvinova, V.V., Deschamps, A., Dugarmaa, T., Deverchére, J., Ulziibat, M., Sankov, V.A., Artem'ev, A.A., Perrot, J. 2007. Velocity structure of the lithosphere on the 2003 Mongolian-Baikal transect from SV waves. Izvestiya, Physics of the

Solid Earth 43, 119-129. https://doi.org/10.1134/S1069351307020036

Nesbitt, H.W., Young, G.M. 1982. Early Proterozoic Climate and Plate Motion Inferred from Major Element Chemistry of lutites. Nature, 299, 715 - 71. https://doi.org/10.1038/299715a0

Pei, F.-P., Xu, W.-L., Yang, D.-B., Ji, W.-Q., Yu, Y., Zhang, X.-Zh. 2008. Mesozoic Volcanic Rocks in the Southern Songliao Basin: Zircon U-Pb Ages and Their Constraints on the Nature of Basin Basement College of Earth Sciences, Jilin University, Changchun 130061, China.

Putirka, K. 1999a. Melting depth and mantle heterogeneity beneath Hawaii and the East Pacific Rise: constraints from Na/Ti and rare earth element ratios. Journal of Geophysical Research 104, 2817- 2829. https://doi.org/10.1029/1998JB900048

Putirka, K. 1999b. Clinopyroxene+liquid equilibria to 100 kbar and 2450 K. Contributions to Mineralogy and Petrology 135, 151- 163. https://doi.org/10.1007/s004100050503

Rasskazov, S.V., Saranina, E.I., Demonterova, E.I., Maslovskaya, M.N., Ivanov, A.V. 2002. Mantle components in Late Cenozoic volcanics, East Sayan (from Pb, Sr, and Nd isotopes). Russian Geology and Geophysics 43, 1065-1079.

Rowley, D.B. 1996. Age of initiation of collision between India and Asia: A review of stratigraphic data. Earth and Planetary Science Letters 145, 1-13. https://doi.org/10.1016/S0012-821X(96)00201-4

Ryu, S., Oka, M., Yagi, K., Sakuyama, T., Itaya, T. 2011. K-Ar ages of the Quaternary basalts in the Jeongok area, the central part of Korean Peninsula. Geosciences Journal 15, 1-8. https://doi.org/10.1007/s12303-011-0008-x

Sengör, A.M., Natal'in, B.A. 1996. Paleotectonics of Asia: Fragments of a Synthesis. Tectonic Evolution of Asia 21, 486-640.

Stracke, A., Bizimis, M., Salters, V.M. 2003. Recycling oceanic crust: Quantitative constraints: RECYCLING OCEANIC CRUST. Geochemistry Geophysics Geosystems 4, 8003. https://doi.org/10.1029/2001GC000223

Stracke, A., Hofmann, A.W., Hart, S.R., 2005. FOZO, HIMU, and the rest of the mantle zoo. Geochemistry, Geophysics, Geosystems 6. https://doi.org/10.1029/2004GC000824

Sun, M.D., Chen, H.L., Zhang, F.Q., Wilde, S.A., Dong, C.W., Yang, S.F. 2013. A 100 Ma bimodal composite dyke complex in the Jiamusi Block, NE China: An indication for lithospheric extension driven by Paleo-Pacific roll-back. Lithos, 162-163, 317-330. https://doi.org/10.1016/j.lithos.2012.11.021

Sun, S.S., McDonough, W.F. 1989. Chemical and isotopic systematics of oceanic basalts: Implications for mantle composition and processes. Geological Society, London, Special Publications 42, 313-345. https://doi.org/10.1144/GSL.SP.1989.042.01.19

Tang, Y.-J., Zhang, H.-F., Ying, J.-F. 2006. Asthenosphere-lithosphere interaction in an extensional regime: Implication from the geochemistry of Cenozoic basalts from Taihang Mountains, North China Craton. Chemical Geology 233, 309-327. https://doi.org/10.1016/j.chemgeo.2006.03.013

Togtokh, Kh., Miao,L., Zhang, Fo., Baatar, Ts., Anaad, Ch., Bars, A. 2018. Major, trace element and Sr-Nd isotopic geochemistry of Cenozoic basalts in Central-North and East Mongolia: Petrogenesis and tectonic implication. Geological journal. https://doi.org/10.1002/gj.3331

Tomurtogoo, O., Windley, B.F., Kröner, A., Badarch, G., Liu, D.Y. 2005. Zircon age and occurrence of the adaatsag ophiolite and Muron shear zone, central Mongolia: constraints on the evolution of the Mongol-Okhotsk ocean, suture and orogen. Geological Society, London 162, 125-134

Wildley, B.F., Allen, M.B. 1993. Mongolian plateau: evidence for a late Cenozoic mantle plume under central Asia. Geology 21, 296-298. https://doi.org/10.1130/0091-7613(1993)021<0295:MPEFAL>2.3.CO;2

Wu, F.Y., Lin, J.Q., Wilde, S.A., Zhang, X.O., Yang, J.H. 2005. Nature and significance of the Early Cretaceous giant igneous event in eastern China. Earth and Planetary Science Letters, 233, 103-119. https://doi.org/10.1016/j.epsl.2005.02.019

Xiao, W., Mao, Q., Windley, B.F. 2010. Paleozoic multiple accretionary and collisional processes of the Beishan orogenic collage. American Journal of Science 310, 1552-1594. https://doi.org/10.2475/10.2010.12

Xu, Y.G. 2014. Recycled oceanic crust in the source of 90-40Ma basalts in North and Northeast China: Evidence, provenance and significance. Geochimica et Cosmochimica Acta 143, 49-67. https://doi.org/10.1016/j.gca.2014.04.045

Xu, Y.-G., Ma, J.-L., Frey, F.A., Feigenson, M.D., Liu, J.-F. 2005. Role of lithosphere-asthenosphere interaction in the genesis of Quaternary alkali and tholeiitic basalts from Datong, western North China Craton. Chemical Geology 224, 247-271. https://doi.org/10.1016/j.chemgeo.2005.08.004

Xu, Y.-G., Zhang, H.-H., Qiu, H.-N., Ge, W.-C., Wu, F.-Y. 2012. Oceanic crust components in continental basalts from Shuangliao, Northeast

China: Derived from the mantle transition zone? Chemical Geology 328, 168-184. https://doi.org/10.1016/j.chemgeo.2012.01.027

Xu, Z., Zheng, Y.-F. 2017. Continental basalts record the crust-mantle interaction in oceanic subduction channel: A geochemical case study from eastern China. Journal of Asian Earth Sciences 145, 233-259. https://doi.org/10.1016/j.jseaes.2017.03.010

Yan, J., Zhao, J.-X. 2008. Cenozoic alkali basalts from Jingpohu, NE China: The role of lithosphere-asthenosphere interaction. Journal of Asian Earth Sciences 33, 106-121. https://doi.org/10.1016/j.jseaes.2007.11.001

Yarmolyuk, V.V., Ivanov, V.G., Kovalenko, V.I., Pokrovskii, B.G., 2003. Magmatism and geodynamics of the Southern Baikal volcanic region (Mantle Hot Spot): results of geochronological, geochemical, and isotopic (Sr, Nd, and O) investigations. Petrology 11, 1-30.

Yarmolyuk, V.V., Kudryashova, E.A., Kozlovsky, A.M., Lebedev, V.A., Savatenkov, V.M. 2015. Late Mesozoic-Cenozoic intraplate magmatism in Central Asia and its relation with mantle diapirism: Evidence from the South Khangai volcanic region, Mongolia. Journal of Asian Earth Sciences 111, 604-623. https://doi.org/10.1016/j.jseaes.2015.05.008

Yarmolyuk, V.V., Kudryashova, E.A., Kozlovsky, A.M., Savatenkov, V.M. 2011. Late Cenozoic volcanic province in Central and East Asia. Petrology 19, 327-347. https://doi.org/10.1134/S0869591111040072

Yin, A. 2010. Cenozoic tectonic evolution of Asia: A preliminary synthesis. Tectonophysics 488, 293-325. https://doi.org/10.1016/j.tecto.2009.06.002

Zhang, F.Q., Chen, H.L., Yu, X., Dong, C.W., Yang, S.F., Pang, Y.M., Batt, G.E. 2011. Early Cretaceous volcanism in northern Songliao Basin, NE China, and its geodynamic implication. Gondwana Research, 19, 163-176. https://doi.org/10.1016/j.gr.2010.03.011

Zhang, L.C., Chen, Z.G., Zhou, X.H., Wang, F., Zhang, Y.T. 2007. Characteristics of deep sources and tectonic-magmatic evolution of the Early Cretaceous volcanics in Ganhe area. Da-Hinggan Mountains of Sr-Nd-Pb-Hf isotopic geochemistries: Acta Petrologica Sinica, 23, 2823-2835 (In Chinese).

Zhang, M., Guo, Z., Cheng, Z., Zhang, L., Liu, J. 2014. Late Cenozoic intraplate volcanismin Changbai volcanic field, on the border of China and North Korea: insights into deep subduction of the Pacific slab and intraplate volcanism. Journal of the Geological Society 172, 648-663. https://doi.org/10.1144/jgs2014-080

Zhang, Q., Willems, H., Ding, L., Gräfe, K.-U., Appel, a.E., 2012. Initial India-Asia Continental Collision and Foreland Basin Evolution in the Tethyan Himalaya of Tibet: Evidence from Stratigraphy and Paleontology. Journal of Geology 120, 175-189. https://doi.org/10.1086/663876

Zhao, D., Tian, Y., Lei, J., Liu, L., Zheng, S. 2009. Seismic image and origin of the Changbai intraplate volcano in East Asia: Role of big mantle wedge above the stagnant Pacific slab. Physics of the Earth and Planetary Interiors 173, 197-206. https://doi.org/10.1016/j.pepi.2008.11.009

Zhou, J.B., Wilde, S.A., Zhang, X.Z., Zhao, G.C., Zheng, C.Q., Wang, Y.J., Zhang, X.H. 2009. The onset of Pacific margin accretion in NE China: Evidence from the Heilongjiang high-pressure metamorphic belt. Tectonophysics, 478, 230-246. https://doi.org/10.1016/j.tecto.2009.08.009

Zhu, B., Kidd, W.S.F., Rowley, D.B., Currie, B.S., Shafique, A.N. 2005. Age of Initiation of the India -Asia Collision in the East-Central Himalaya. Journal of Geology 113, 265-285. https://doi.org/10.1086/428805

Zhu, R., Pan, Y., Shaw, J., Li, D., Li, Q. 2001. Geomagnetic palaeointensity just prior to the Cretaceous normal superchron. Physics of the Earth and Planetary Interiors 128, 207-222. https://doi.org/10.1016/S0031-9201(01)00287-4